An endogenous tumour-promoting ligand of the human aryl hydrocarbon receptor

Opitz, C A ; Litzenburger, U M ; Sahm, F ; Ott, M ; Tritschler, I ; Trump, S ; Schumacher, T ; Jestaedt, L ; Schrenk, D ; Weller, M ; Jugold, M ; Guillemin, G J ; Miller, C L ; Lutz, C ; Radlwimmer, B ; Lehmann, I ; von Deimling, A ; Wick, W ; Platten, M

Abstract: Activation of the aryl hydrocarbon receptor (AHR) by environmental xenobiotic toxic chemicals, for instance 2,3,7,8-tetrachlorodibenzo-p-dioxin (dioxin), has been implicated in a variety of cellular processes such as embryogenesis, transformation, tumorigenesis and inflammation. But the identity of an endogenous ligand activating the AHR under physiological conditions in the absence of environmental toxic chemicals is still unknown. Here we identify the tryptophan (Trp) catabolite kynurenine (Kyn) as an endogenous ligand of the human AHR that is constitutively generated by human tumour cells via tryptophan-2,3-dioxygenase (TDO), a liver- and neuron-derived Trp-degrading enzyme not yet implicated in cancer biology. TDO-derived Kyn suppresses antitumour immune responses and promotes tumour-cell survival and motility through the AHR in an autocrine/paracrine fashion. The TDO-AHR pathway is active in human brain tumours and is associated with malignant progression and poor survival. Because Kyn is produced during cancer progression and inflammation in the local microenvironment in amounts sufficient for activating the human AHR, these results provide evidence for a previously unidentified pathophysiological function of the AHR with profound implications for cancer and immune biology.

DOI: https://doi.org/10.1038/nature10491

An endogenous ligand of the human aryl hydrocarbon receptor promotes tumor formation.

Christiane A. Opitz[1,2*], Ulrike M. Litzenburger[1,2*], Felix Sahm[3], Martina Ott[1,2], Isabel Tritschler[4], Saskia Trump[5], Theresa Schumacher[1,2], Leonie Jestaedt[6], Dieter Schrenk[7], Michael Weller[4], Manfred Jugold[8], Gilles J. Guillemin[9], Christine L. Miller[10], Christian Lutz[11], Bernhard Radlwimmer[12], Irina Lehman[5], Andreas von Deimling[3], Wolfgang Wick[1,13], Michael Platten[1,2]

[1]Department of Neurooncology, Neurology Clinic and National Center for Tumor Diseases University Hospital of Heidelberg, Heidelberg, Germany; [2]Experimental Neuroimmunology Unit, German Cancer Research Center (DKFZ), Heidelberg, Germany; [3]Department of Neuropathology, Institute of Pathology, University Hospital of Heidelberg and Clinical Cooperation Unit Neuropathology, German Cancer Research Center (DKFZ), Heidelberg, Germany, [4]Department of Neurology, University Hospital Zürich, Zurich, Switzerland; [5]Department for Environmental Immunology, Helmholtz Center for Environmental Research, Leipzig, Germany; [6]Department of Neuroradiology, University Hospital of Heidelberg, Germany; [7]Food Chemistry and Toxicology, University of Kaiserslautern, Kaiserslautern, Germany; [8]Small Animal Imaging Center, German Cancer Research Center (DKFZ), Heidelberg, Germany; [9]Department of Pharmacology, University of New South Wales, Sydney, Australia; [10]Department of Pediatrics, Johns Hopkins University, Baltimore, MD, USA [11]Heidelberg Pharma AG, Ladenburg, Germany; [12]Department of Molecular Genetics, German Cancer Research Center (DKFZ), Heidelberg, Germany; [13]Clinical Cooperation Unit Neurooncology, German Cancer Research Center (DKFZ), Heidelberg, Germany

* these authors contributed equally to this work

Word count: 3086, summary paragraph: 170, figures: 6, references: 34

Activation of the aryl hydrocarbon receptor (AHR) by environmental xenobiotic toxins, for instance 2,3,7,8-tetrachlorodibenzo-p-dioxin (dioxin), has been implicated in a variety of cellular processes such as embryogenesis, transformation, tumorigenesis and inflammation. The identity of an endogenous ligand activating the AHR under physiological conditions in the absence of environmental toxins, however, has remained enigmatic. We identify the tryptophan (Trp) catabolite kynurenine (Kyn) as an endogenous ligand of the human AHR that is constitutively generated by human tumor cells via tryptophan-2,3-dioxygenase (TDO), a liver- and neuron-specific Trp-degrading enzyme not yet implicated in cancer biology. TDO-derived Kyn suppresses antitumor immune responses and promotes tumor cell survival and motility via the AHR in an autocrine/paracrine fashion. The TDO-AHR pathway is active in human brain tumors and associated with malignant progression and poor survival. As Kyn is produced during cancer progression and inflammation in the local microenvironment in amounts sufficient for activating the human AHR, these results provide evidence for a novel pathophysiological function of the AHR with profound implications for cancer and immune biology.

Degradation of Trp by indoleamine-2,3-dioxygenases 1 and 2 (IDO1/2) in tumors and tumor-draining lymph nodes inhibits antitumor immune responses[1-5] and is associated with a poor prognosis in various malignancies[6]. Inhibition of IDO1/2 suppresses tumor formation in animal models[1,3] and is currently tested in phase I/II clinical trials in cancer patients[7]. The relevance of Trp catabolism for human tumor formation and progression however remains elusive. A screen of human cancer cell lines revealed constitutive degradation of Trp and release of high micromolar amounts of Kyn in brain tumor cells, namely glioma cell lines and glioma-initiating cells (GIC), but not human astrocytes (Fig. 1a). Surprisingly, IDO1 and

IDO2 did not account for the constitutive Trp catabolism in brain tumors (Supplementary Fig. 1a-e, Supplementary note 1). Conversely, tryptophan-2,3-dioxygenase (TDO), which is predominantly expressed in the liver and believed to regulate systemic Trp concentrations[6], was strongly expressed in human glioma cells (Supplementary Fig. 1b) and correlated with Kyn release (Fig. 1b; Supplementary note 2). Pharmacological inhibition or knockdown of *TDO* blocked Kyn release by glioma cells, while knockdown of *IDO1* and *IDO2* had no effect (Fig. 1c,d, Supplementary Fig. 2a, Supplementary note 3), thus confirming that TDO is the central Trp-degrading enzyme in human glioma cells. In human brain tumor specimens TDO protein expression increased with malignancy and correlated with the proliferation index (Fig. 1e-h, Supplementary Fig. 2b,c,3a,b; Supplementary note 4,5). As described previously[8], healthy human brain showed weak TDO staining in the neurons (Fig. 1e). TDO expression was not confined to gliomas but was also detected in other types of cancers (Supplementary Fig. 3b,c; Supplementary note 6). Reduced Trp concentrations were measured in the sera of glioma patients (Fig. 1i). This enhanced systemic Trp degradation, however, did not translate into increased Kyn levels (Fig. 1i), most likely because Kyn is taken up by other cells and metabolised to quinolinic acid. Indeed, accumulation of quinolinic acid was detected in TDO-expressing glioma tissue (Fig. 1j, Supplementary Fig. 3d; Supplementary note 7).

Kyn suppresses allogeneic T cell proliferation[9]. Allogeneic T cell proliferation inversely correlated with the Kyn formation by glioma-derived TDO (Fig. 2a, Supplementary Fig. 4a,b; Supplementary note 8). Knockdown of *TDO* in glioma cells (Supplementary Fig. 4c,d; Supplementary note 9) restored allogeneic T cell proliferation, while addition of Kyn to the *TDO* knockdown cells prevented the restoration of T cell proliferation (Fig. 2b). Kyn concentration-dependently inhibited the proliferation of T cell receptor stimulated CD4+ and CD8+ T cells (Supplementary Fig. 4e). In addition, knockdown of *TDO* resulted in enhanced lysis of glioma cells by alloreactive PBMC (Supplementary Fig. 4f). Finally, decreased

infiltration with leukocyte common antigen (LCA) positive and CD8+ immune cells was observed in sections of human glioma with high TDO expression in comparison to those with low TDO expression (Fig. 2c,d), indicating that Kyn formation by TDO may suppress antitumor immune responses. *In vivo* experiments in immunocompetent mice demonstrated that tumors expressing TDO grew faster than their TDO-deficient counterparts (Fig 2e; Supplementary Fig. 4g,h; Supplementary Note 10). In line with this result, TDO expressing tumors displayed a higher proliferation index than TDO-deficient controls (Fig. 2f; Suppl. Fig. 4i). TDO activity suppressed antitumor immune responses as evidenced by reduced interferon-gamma (IFN-γ) release of T cells and tumor cell lysis by spleen cells of mice bearing TDO-expressing tumors in comparison with mice bearing TDO-deficient tumors (Fig. 2g,h), thus underscoring that TDO activity suppresses antitumor immune responses *in vivo*.

We next assessed the autocrine effects of Kyn on glioma cells. While no differences in cell cycle progression were detected between controls and glioma cells with *TDO* knockdown (Supplementary Fig. 5a), knockdown of *TDO* reduced motility and clonogenic survival (Fig. 3a-c, Supplementary Fig. 5b,c; Supplementary Note 11). This was mediated by Kyn as exogenous addition of Kyn restored motility and clonogenic survival in the absence of Trp (Fig. 3d,e; Supplementray Fig. 5d,e), suggesting that Kyn increases the motility of malignant glioma cells. In GIC sphere formation was enhanced in response to Kyn (Fig. 3f). Finally, tumor formation was impaired when TDO knockdown tumors were orthotopically implanted in the brains of nude mice, which are devoid of functional T cells (Fig. 3g, Supplementary Fig. 5f,g; Supplementary note 12). To analyse whether inhibition of antitumor NK cell responses, which are functional in nude mice, by TDO may account for impaired formation of *TDO* knockdown tumors, we compared subcutaneous tumor growth in the presence or absence of NK cells. NK cell depletion (Supplementary Fig. 5h) enhanced the growth of both control and *TDO* knockout tumors but did not restore the growth of *TDO* knockout tumors to

that of controls (Fig. 3h). Histochemical analyses revealed that *TDO* knockout tumors showed less mitoses and Ki-67 staining than control tumors (Fig. 3i). Collectively, these data suggest that Kyn generated by constitutive TDO activity enhances the malignant phenotype of human gliomas in an autocrine manner in the absence of functional antitumor T cell and NK cell responses.

To understand the molecular mechanisms underlying the autocrine effects of Kyn on glioma cells, we performed a microarray analysis of Kyn-treated glioma cells. Detailed pathway analysis revealed broad induction of AHR response genes by Kyn (Fig. 4a ; Supplementary Fig. 6a,b, 7; Supplementary note 13). TCDD-inducible poly [ADP-ribose] polymerase (*TIPARP*) and plasminogen activator inhibitor 2 (referred to as *PAI-2* or *SERPINB2*), two direct AHR target genes, showed the strongest upregulation after 24 h (Supplementary Fig. 6a)[10-12]. These two AHR target genes in addition to another direct AHR target gene, cytochrome P450, family 1, subfamily B, polypeptide 1 (*CYP1B1*) were also among the 6 most upregulated genes after 8 h (Supplementary Fig. 6a)[10,11]. The 25 genes with the lowest (array) p-values in response to 8 h and 24 h Kyn are regulated by the AHR (Fig. 4a; Supplementary. Fig. 6b). The AHR is a transcription factor of the basic helix-loop-helix (bHLH) Per-Arnt-Sim (PAS) family, which is activated by xenobiotics such as benzo[*a*]pyrene and 2,3,7,8-tetrachlordibenzodioxin (TCDD)[13]. Malignant glioma cell lines as well as GIC express the AHR constitutively (Supplementary Fig. 6c)[14], and upregulation of AHR target genes by Kyn was confirmed in two different glioma cell lines (Supplementary Fig. 6d,e). Kyn led to translocation of the AHR into the nucleus after 1 h, thus showing an immediate effect of Kyn on the AHR (Fig. 4b,c, Supplementary Fig. 8a). In accordance, Western blot analyses of Kyn-activated tumor cells showed reduced cytoplasmic localisation paralleled by increased nuclear accumulation of the AHR comparable to that induced by TCDD (Fig. 4d). In the nucleus the AHR forms a heterodimer with the AHR nuclear

translocator (ARNT) that interacts with the core binding motif of the dioxin-response elements (DRE) located in regulatory regions of AHR target genes[15]. Kyn concentration-dependently induced DRE-luciferase activity in glioma cells with an EC50 of 36.6 µM (Fig. 4e). AHR activation was unique to Kyn in a panel of Trp catabolites (Supplementary Table 1). An ethoxyresorufin-O-deethylase (EROD) assay confirmed the induction of the functional AHR target gene cytochrome P450, family 1, subfamily A, polypeptide 1 (CYP1A1) with an EC50 of 12.3 µM for Kyn (Supplementary Fig. 8b). Radioligand binding assays using mouse liver cytosol from *Ahr*-proficient and *Ahr*-deficient mice demonstrated that Kyn binds to the AHR with a $K_D^{(app)}$ of ≈ 4 µM (Fig. 4f).

The activation of the AHR and upregulation of AHR-regulated gene expression in response to Kyn was inhibited by the AHR antagonist 3,4-DMF (Fig. 4g, Supplementary Fig. 8f,g; Supplementary note 14) or knockdown of the *AHR* (Fig. 4h,i, Supplementary Fig. 8h,i), indicating that Kyn is a specific agonist of the AHR. The involvement of the same or similar AHR residues in the binding to Kyn, TCDD and 3-MC was confirmed by the fact that activation of the AHR by all three ligands was inhibited by 3,4-DMF (Supplementary Fig. 8f,g; Supplementary note 14). Importantly, the endogenous Kyn production of glioma cells was sufficient to activate the AHR, as knockdown of *TDO* decreased the expression of AHR regulated genes (Fig. 4j, Supplementary Fig. 8j,k; Supplementary note 15). As mean Kyn concentrations of 37.01 +/- 13.4 µM were measured in U87 xenografts (n=6), sufficient Kyn concentrations to activate the AHR were also reached *in vivo* (Suplementary note 15).

We next assessed whether the tumor-promoting effects of Kyn are mediated by the AHR. Kyn failed to induce motility of glioma cells after *AHR* knockdown (Fig. 5a). Also, the increase in clonogenic survival in response to Kyn was abolished in glioma cells with a knockdown of the *AHR* (Fig. 5b,c). Interleukin 1, beta *(IL1B)*, epiregulin *(EREG)*, aldehyde dehydrogenase 1 family, member A3 *(ALDH1A3)*, interleukin 8 *(IL8)* and interleukin 6 *(IL6)* are regulated by

Kyn via the AHR in glioma cells and have been reported to promote invasiveness and tumor growth, suggesting that these genes may contribute to the autocrine tumor-promoting effects of TDO-derived Kyn (Supplementary Note 16). In summary these data indicate that AHR signaling is indeed responsible for the autocrine effects of TDO-derived Kyn on tumor cells.

To determine whether TDO also influences antitumor immune responses via the AHR we analysed the infiltration of LCA+ and CD8+ immune cells in human glioma sections in relation to their AHR expression (Fig. 5d,e). Infiltration by LCA+ and CD8+ immune cells was decreased in sections of human glioma with high AHR expression compared to those with low AHR expression (Fig. 5d,e), suggesting that AHR signalling may be involved in reducing immune cell infiltration. In accordance with an activation of the AHR by TDO-derived Kyn, expression of the AHR target gene TIPARP in LCA+ immune cells was observed only in sections expressing TDO (Fig. 5f). To analyse the contribution of host AHR expression to tumor growth, we compared the growth of murine tumors with and without *Tdo* expression in *Ahr*-deficient and *Ahr*-proficient mice. In *Ahr*-proficient mice *Tdo* expression strongly enhanced tumor growth in comparison to tumors not expressing *Tdo* (Fig. 5g). The same effect was observed in *Ahr*-deficient mice, albeit to a much lower extent (Fig. 5g). As murine glioma cells express functional AHR (Supplementary Fig. 9a, Supplementary note 17), these results suggest that the increase in tumor growth mediated by TDO in *Ahr*-deficient mice is due to autocrine effects of TDO on the tumor cells themselves. The finding that TDO leads to stronger tumor growth in *Ahr*-proficient than in *Ahr*-deficient mice (Fig. 5g), indicates that AHR-mediated host effects enhance tumor growth. Staining of LCA+ immune cells in the tumors revealed that expression of TDO reduced the infiltration with LCA+ immune cells in *Ahr*-proficient mice, but not in *Ahr*-deficient mice (Fig. 5h,i), suggesting that TDO-mediated suppression of anti-tumor immune responses via the AHR contributes to the host effects enhancing the growth of *Tdo*-expressing tumors. In summary, these results

indicate that TDO enhances tumor growth by suppressing the antitumor immune response via the AHR.

To assess the effect of AHR activity on the tumor cells themselves, we performed *in vivo* experiments using *AHR*-proficient and *AHR*-deficient human glioma cells (Fig 5j). Knockdown of the *AHR* in the glioma cells inhibited tumor growth (Fig.5j, Supplementary note 18), underscoring the importance of AHR signaling for the autocrine effects of Trp degradation. In line, the *AHR* knockdown tumors showed less mitoses and a reduced proliferative index in comparison to the *AHR*-proficient control tumors (Fig.5k).

Next we aimed to investigate whether TDO-derived Kyn activates the AHR in human brain tumor tissue. Indeed, TDO expression correlated with the expression of the AHR and AHR target genes in human glioma tissue (Fig. 6a-d, Supplementary Fig.9d,e; Supplementary note 19), indicating that constitutive TDO expression in glioma cells produced sufficient Kyn levels to activate the AHR. To address whether the TDO-Kyn-AHR signalling pathway is also activated in cancers other than gliomas, we analysed microarray data of diverse human tumor entities (Fig. 6e; Supplementary Fig. 10a). Interestingly, *TDO* expression correlated with the expression of the AHR target gene *CYP1B1* not only in glioma (Fig. 6d), but also in B cell lymphoma, Ewing sarcoma, bladder carcinoma, cervix carcinoma, colorectal carcinoma, lung carcinoma and ovarian carcinoma (Fig. 6e; Supplementary. Fig. 10a; Supplementary note 20). This finding indicates that the TDO-Kyn-AHR pathway is not confined to brain tumors but appears to be a common trait of cancers.

Analysis of the Rembrandt database revealed that the overall survival of glioma patients (WHO grade II-IV) with an upregulation of *TDO*, the *AHR* or the AHR target gene *CYP1B1* was reduced compared to patients with intermediate or downregulated expression of these genes (Fig. 6f; Supplementary Fig. 10b; Supplementary note 21)[16]. Finally, in patients with

glioblastoma (WHO grade IV)[17], the expression of the AHR targets *CYP1B1*, *IL1B*, *IL6* and *IL8*, which are regulated by TDO-derived Kyn in glioma cells (Fig. 4j; Supplementary Fig. 6d,e), were found to predict survival even independent of WHO grade (Fig. 6g; Supplementary Fig. 10c), thus further underscoring the importance of AHR activation for the malignant phenotype of gliomas. In summary these data suggest that endogenous tumor-derived Kyn activates the AHR in an autocrine/paracrine fashion to promote tumor progression.

Cancer-associated immunosuppression by Trp degradation has to date been attributed solely to the enzymatic activity of IDO in cancer cells and tumor-draining lymph nodes. Thus, IDO inhibition is currently being evaluated as a therapeutic strategy to treat cancer in clinical trials[7]. We show that TDO is strongly expressed in cancer and equally capable of producing immunosuppressive Kyn. In IDO-negative glioma cells, TDO appears to be the sole determinant of constitutive Trp degradation, indicating that TDO represents a novel therapeutic target in glioma therapy. Furthermore we delineate the importance of constitutive Trp degradation to sustain the malignant phenotype of cancer by acting on the tumor cells themselves.

Emerging evidence points towards a tumor-promoting role of the AHR. AHR activation promotes clonogenicity and invasiveness of cancer cells[14,18]. Transgenic mice with a constitutively active AHR spontaneously develop tumors[19,20] and the repressor of the AHR (AHRR) is a tumor suppressor gene in multiple human cancers[21]. The aberrant phenotype of *Ahr*-deficient mice points to the existence of endogenous AHR ligands[22]. While different endogenously produced metabolites such as arachidonic acid metabolites, bilirubin, cAMP, tryptamine and 6-formylindolo[3,2-b]carbazole (FICZ) have been shown to be agonists of the AHR[23], their functionality has not been convincingly demonstrated in a pathophysiological

context such as cancer or immune activation. The search for endogenous ligands of the AHR therefore is ongoing.

We now link these two important pathways contributing to cancer progression by showing that Trp catabolism leads to AHR activation and provide evidence of a pathophysiological human condition that is associated with the production of sufficient amounts of a functionally relevant endogenous AHR ligand. Our results reveal a differential response of primary immune cells and transformed cancer cells to AHR-mediated signals, which is in line with various toxicological studies using the classical exogenous AHR ligands, TCDD and 3-MC[14,18,24]. Exposure to these xenobiotics leads to profound suppression of cellular and humoral immune responses[24], while also promoting carcinogenesis and inducing tumor growth[14,18]. These cell-specific differences in AHR effects are likely to depend on the expression of factors differentially regulating AHR signal transduction such as the AHRR[21] as well as cell-specific transcription factor crosstalk shaping the response to AHR activation[25].

It is likely that Kyn-mediated activation of the AHR is not only relevant in the setting of cancer. For instance, activation of the mouse and human AHR by agonistic ligands induces regulatory T cells[26-29]. Interestingly, *Ahr*-deficient mice suffer from exacerbated CNS autoimmunity in the absence of an exogenous ligand[27], while Trp catabolites suppress CNS autoimmunity[30], suggesting that activation of Trp catabolism represents an endogenous feed-back loop to restrict inflammation via the AHR. In fact, exogenous Kyn is involved in the regulation of immune cells in mice via the AHR[31,32]. Kyn concentrations sufficient to activate the AHR are also generated by IDO in response to inflammatory stimuli (Supplementary Fig. 11a-c; Supplementary note 22). In a broader context, a significant number of malignancies arise from areas of mostly chronic infection and inflammation[33], where Trp catabolism in the tumor microenvironment is activated and sustains local immune suppression[34]. Activation of

the AHR by Kyn generated in response to inflammatory stimuli may thus constitute a previously unrecognized pathway connecting inflammation and carcinogenesis.

Methods Summary

TDO expression was analysed by immunohistochemistry in human tumors. Its relevance for Trp degradation was determined using genetic knockdown or overexpression of TDO. Trp and Kyn were measured in cell culture supernatants, human sera and xenograft tissue by HPLC. Mixed leukocyte reactions, chromium release, Elispot and staining of immune cells in tumor tissues were used to access the immune effects of TDO activity. Cell cycle analysis, matrigel and spheroid invasion assays, scratch assays, sphere formation assays and clonogenic survival assays were employed to analyse the autocrine effects of TDO activity. Orthotopic implantation of human glioma cells with and without stable knockdown of *TDO* into *CD1nu/nu* mice, s.c. injection of these cells into NK-depleted or wildtype *CD1nu/nu* mice and s.c. injection of murine *Tdo*-proficient and *Tdo*-deficient GL261 cells into syngeneic C57BL/6N mice were performed to analyse the autocrine and paracrine effects of TDO activity *in vivo*. Microarray analysis of Kyn-treated human glioma cells was performed to identify signalling pathways activated by Kyn. Analysis of AHR translocation, DRE-luciferase assays and radioligand binding assays confirmed activation of the AHR by Kyn. Pharmacological inhibition and stable knockdown of the AHR (*in vitro* and in *vivo*) proved that the effects of Kyn are AHR-dependent. Injection of *Tdo*-proficient and *Tdo*-deficient tumor cells into *Ahr*+/+ and *Ahr*-/- mice was used to address the contribution of host effects to TDO-mediated cancer promotion. Finally stainings, mircoarray data and clinical data of human tumor tissues were used to analyse whether TDO activates the AHR in human cancers and how this affects survival.

Full Methods and any associated references are available in the online version of the paper at www.nature.com/nature

References

1 Muller, A. J. et al., Inhibition of indoleamine 2,3-dioxygenase, an immunoregulatory target of the cancer suppression gene Bin1, potentiates cancer chemotherapy. *Nat Med* 11 (3), 312 (2005).

2 Munn, D. H. and Mellor, A. L., Indoleamine 2,3-dioxygenase and tumor-induced tolerance. *J Clin Invest* 117 (5), 1147 (2007).

3 Uyttenhove, C. et al., Evidence for a tumoral immune resistance mechanism based on tryptophan degradation by indoleamine 2,3-dioxygenase. *Nat Med* 9 (10), 1269 (2003).

4 Ball, H. J. et al., Characterization of an indoleamine 2,3-dioxygenase-like protein found in humans and mice. *Gene* 396 (1), 203 (2007).

5 Metz, R. et al., Novel tryptophan catabolic enzyme IDO2 is the preferred biochemical target of the antitumor indoleamine 2,3-dioxygenase inhibitory compound D-1-methyl-tryptophan. *Cancer Res* 67 (15), 7082 (2007).

6 Lob, S. et al., Inhibitors of indoleamine-2,3-dioxygenase for cancer therapy: can we see the wood for the trees? *Nat Rev Cancer* 9 (6), 445 (2009).

7 NewLink Genetics Corporation. IDO Inhibitor Study for Relapsed or Refractory Solid Tumors (D-1MT). In: ClinicalTrials.gov [Internet]. Bethesda (MD): National Library of Medicine (US). 2000- [cited 2010 Oct 20]. Available from: http://clinicaltrials.gov/show/NCT00004451 NLM Identifier: NCT00004451.

8 Miller, C. L. et al., Expression of the kynurenine pathway enzyme tryptophan 2,3-dioxygenase is increased in the frontal cortex of individuals with schizophrenia. *Neurobiol Dis* 15 (3), 618 (2004).

9 Frumento, G. et al., Tryptophan-derived catabolites are responsible for inhibition of T and natural killer cell proliferation induced by indoleamine 2,3-dioxygenase. *J Exp Med* 196 (4), 459 (2002).

10 Alexander, D. L., Eltom, S. E., and Jefcoate, C. R., Ah receptor regulation of CYP1B1 expression in primary mouse embryo-derived cells. *Cancer Res* 57 (20), 4498 (1997).

11 Dohr, O., Vogel, C., and Abel, J., Different response of 2,3,7,8-tetrachlorodibenzo-p-dioxin (TCDD)-sensitive genes in human breast cancer MCF-7 and MDA-MB 231 cells. *Arch Biochem Biophys* 321 (2), 405 (1995).

12 Ma, Q. et al., TCDD-inducible poly(ADP-ribose) polymerase: a novel response to 2,3,7,8-tetrachlorodibenzo-p-dioxin. *Biochem Biophys Res Commun* 289 (2), 499 (2001).

13 Denison, M. S. and Nagy, S. R., Activation of the aryl hydrocarbon receptor by structurally diverse exogenous and endogenous chemicals. *Annu Rev Pharmacol Toxicol* 43, 309 (2003).

14 Gramatzki, D. et al., Aryl hydrocarbon receptor inhibition downregulates the TGF-beta/Smad pathway in human glioblastoma cells. *Oncogene* 28 (28), 2593 (2009).

15 Reyes, H., Reisz-Porszasz, S., and Hankinson, O., Identification of the Ah receptor nuclear translocator protein (Arnt) as a component of the DNA binding form of the Ah receptor. *Science* 256 (5060), 1193 (1992).

16 National Cancer Institute 2005 REMBRANDT home page. http://rembrandt.nci.nih.gov acessed 2010 October 20.

17 The Cancer Genome Atlas Research Network, Comprehensive genomic characterization defines human glioblastoma genes and core pathways. *Nature* 455 (7216), 1061 (2008).

18 Bui, L. C. et al., Nedd9/Hef1/Cas-L mediates the effects of environmental pollutants on cell migration and plasticity. *Oncogene* 28 (41), 3642 (2009).

[19] Andersson, P. et al., A constitutively active dioxin/aryl hydrocarbon receptor induces stomach tumors. *Proc Natl Acad Sci U S A* 99 (15), 9990 (2002).

[20] Moennikes, O. et al., A constitutively active dioxin/aryl hydrocarbon receptor promotes hepatocarcinogenesis in mice. *Cancer Res* 64 (14), 4707 (2004).

[21] Zudaire, E. et al., The aryl hydrocarbon receptor repressor is a putative tumor suppressor gene in multiple human cancers. *J Clin Invest* 118 (2), 640 (2008).

[22] Fernandez-Salguero, P. et al., Immune system impairment and hepatic fibrosis in mice lacking the dioxin-binding Ah receptor. *Science* 268 (5211), 722 (1995).

[23] Nguyen, L. P. and Bradfield, C. A., The search for endogenous activators of the aryl hydrocarbon receptor. *Chem Res Toxicol* 21 (1), 102 (2008).

[24] Esser, C., Rannug, A., and Stockinger, B., The aryl hydrocarbon receptor in immunity. *Trends Immunol* 30 (9), 447 (2009).

[25] Frericks, M., Burgoon, L. D., Zacharewski, T. R., and Esser, C., Promoter analysis of TCDD-inducible genes in a thymic epithelial cell line indicates the potential for cell-specific transcription factor crosstalk in the AhR response. *Toxicol Appl Pharmacol* 232 (2), 268 (2008).

[26] Apetoh, L. et al., The aryl hydrocarbon receptor interacts with c-Maf to promote the differentiation of type 1 regulatory T cells induced by IL-27. *Nat Immunol* 11 (9), 854.

[27] Quintana, F. J. et al., Control of T(reg) and T(H)17 cell differentiation by the aryl hydrocarbon receptor. *Nature* 453 (7191), 65 (2008).

[28] Quintana, F. J. et al., An endogenous aryl hydrocarbon receptor ligand acts on dendritic cells and T cells to suppress experimental autoimmune encephalomyelitis. *Proc Natl Acad Sci U S A* 107 (48), 20768 (2010).

[29] Veldhoen, M. et al., The aryl hydrocarbon receptor links TH17-cell-mediated autoimmunity to environmental toxins. *Nature* 453 (7191), 106 (2008).

[30] Platten, M. et al., Treatment of autoimmune neuroinflammation with a synthetic tryptophan metabolite. *Science* 310 (5749), 850 (2005).

[31] Mezrich, J. D. et al., An Interaction between Kynurenine and the Aryl Hydrocarbon Receptor Can Generate Regulatory T Cells. *J Immunol* 185 (6), 3190 (2010).

[32] Nguyen, N. T. et al., Aryl hydrocarbon receptor negatively regulates dendritic cell immunogenicity via a kynurenine-dependent mechanism. *Proc Natl Acad Sci U S A* 107 (46), 19961 (2010).

[33] Coussens, L. M. and Werb, Z., Inflammation and cancer. *Nature* 420 (6917), 860 (2002).

[34] Muller, A. J. et al., Chronic inflammation that facilitates tumor progression creates local immune suppression by inducing indoleamine 2,3 dioxygenase. *Proc Natl Acad Sci U S A* 105 (44), 17073 (2008).

Supplementary Information is linked to the online version of the paper at

www.nature.com/nature.

Acknowledgements

We thank Katharina Rauschenbach, Jennifer Reiert, Sabrina Koch and Andreas Mlitzko for technical assistance, Philipp Pfenning for help with the invasion assays, Jonas Blaes for help generating genetically modified cells, Tobias V. Lanz and Iris Oezen for help with animal experiments, Michael Schwarz for providing the human DRE-luciferase construct, Katharina Ochs for providing HUVEC cDNA, Anne Hertenstein for generation of CD4+ and CD8+ T cells, Matthew Batts and Robert Russel for AHR ligand modeling, Rainer Koch for performing qRT-PCR analyses, Ruxandra Tudoran for generation of GL261 cells overexpressing murine TDO, Marcel Deponte for help with the radioligand binding assay, Daniela Schemmer for collecting and banking serum samples, Wilfried Roth for providing tissue specimens, Marc Remke for suggestions regarding data analysis and Günter Hämmerling for helpful discussions. This work was supported by grants from the Helmholtz Association (VH-NG-306) to MP, the German Research Foundation to MP and WW (DFG SFB 938 TP K), the Hertie Foundation to WW and the Helmholtz Alliance on Systems Biology to ST and IL. TS is supported by a DKFZ PhD Program stipend, CAO is supported by a Heidelberg University Medical Faculty Postdoctoral Fellowship.

Author contributions

C.A.O. and U.M.L. contributed equally to this study, they performed and designed experiments, analysed data and wrote the paper; F.S. and A.D analysed protein expression by immunohistochemistry; I. T. cloned constructs and designed experiments; S.T. and I.L. performed nuclear translocation assays; M.O. performed animal experiments; T.S performed immune experiments; L.J and M.J. performed MRI scans; C.L.M and G.J.G. provided antibodies and designed experiments; D.S. performed and analysed EROD and DRE-luciferase assays; C.L. synthesized the TDO inhibitor; M.W. and W.W. were involved in study design and data interpretation; B.R. analysed miroarray data; M.P. interpreted data,

designed experiments and wrote the paper. All authors discussed the results and commented on the manuscript.

Data deposition: Microarray data were deposited in the Gene Expression Omnibus repository (GEO) at www.ncbi.nlm.nih.gov/geo/ under accession number GSE25272.

The authors declare no competing financial interests.

Correspondence and requests for materials should be addressed to M.P. (m.platten@dkfz-heidelberg.de)

Figure Legends

Figure 1 TDO degrades Trp to Kyn in human brain tumors. **a,** Trp (left) and Kyn (right) content in the supernatants of human astrocytes (hAs), glioma cell lines and GIC (T323) cultured for 72 h and measured by HPLC (n=4). **b,** Correlation between *TDO* mRNA and Kyn release of human glioma cells measured by quantitative RT-PCR and HPLC (n=4). **c,** Kyn concentrations in the supernatants of U87 glioma cells cultured for 48 h in the presence of the TDO inhibitor 680C91 (black bars), controls (white bars; n=4, P= 0.005, 0.002 and 0.0009 for 1, 5 and 10 µM TDOI, respectively). **d,** Kyn release of glioma cells after knockdown of *TDO* (black bars, P = 0.000007, 0.0007 and 0.00006, respectively), *IDO1* (dark gray bars) or *IDO2* (light gray bars) by siRNA. (n=3) **e,** Weak neuronal TDO expression in healthy brain tissue (upper panel). TDO expression in glioblastoma (WHO grade IV, lower panel); red: TDO staining; * necrosis; arrowheads: border to infiltrated brain tissue. Inset: single tumor cells (arrows) infiltrating the adjacent brain tissue. Magnification: 40x, insets 100x. **f,** TDO expression in human glioma sections of different WHO grades. Upper panel: astrocytoma grade II (left), astrocytoma grade III (right). Lower panel: oligodendroglioma grade II (left), oligodendroglioma grade III (right). Magnification 40x. **g,** Plot of TDO expression [H-score] in brain tumors of increasing malignancy (WHO grade II- IV; grade II n=18, grade III n=15, grade IV=35). **h,** Correlation of the Ki-67 proliferative index with the TDO H-score in gliomas of different WHO grades (n = 42). P = 3.169^{-8}. **i,** Trp (left) and Kyn (right) concentrations in the sera of 24 glioblastoma patients and 24 age- and sex-matched healthy controls, measured by HPLC. **j,** Quantification of quinolinic acid staining in healthy human brain tissue (white bar, n=5) and glioblastoma tissue (black bar, n=5). The data distribution in **(g)** and **(i)** is presented using box plots, showing the 25th and 75th percentile together and the median, whiskers represent the 10th and 90th percentile, respectively.

Figure 2 Paracrine effects of TDO-mediated Kyn release by glioma cells on immune cells.

a, Correlation of the allogeneic proliferation of PBMC cocultured with different glioma cell lines with the Kyn release of the glioma cells (n=3). **b,** Allogeneic proliferation of PBMC cocultured with *TDO*-expressing control U87 glioma cells (sh-c) in comparison to U87 glioma cells with a stable short hairpin RNA-mediated knockdown of *TDO* (sh-*TDO*) (blackbars), with or without 100 µM Kyn, in comparison to PBMC alone (white bars, n=3). **c,** Quantification of LCA+ cells stained in human glioma sections with low TDO expression (Histoscore < 150, white bar, n=12) and in human glioma sections with high TDO expression (Histoscore ≥ 150, black bar, n=17). **d,** Quantification of CD8+ cells stained in human glioma sections with low TDO expression (Histoscore < 150, white bar, n=10) and in human glioma sections with high TDO expression (Histoscore ≥ 150, black bar, n=10). **e,** Growth of *Tdo*-expressing (solid circles) and *Tdo*-deficient control (open circles) GL261 murine glioma cells injected s.c. into the flank of C57BL/6N mice was monitored using metric callipers (n=6). Tumor weight was calculated using to the equation: tumor weight (g) = (length (cm) × width $(cm)^2$) × 0.5. **f,** Representative TDO and Ki-67 staining of *Tdo*-expressing (upper panels) and control GL261 tumors (lower panels). **g,** Interferon-gamma release of T cells of mice with a subcutaneous *Tdo*-expressing tumor (black bar) in comparison to those with a subcutaneous *Tdo*-deficient tumor (white bar) in the presence of glioma lysates measured by Elispot (n=3). **h,** Lysis of GL261 murine glioma cells by spleen cells of mice with a *Tdo*-expressing subcutaneous GL261 tumor in comparison to those with a subcutaneous *Tdo*-deficient GL261 tumor meausured by chromium release (n=4).

Figure 3 Autocrine effects of TDO-mediated Kyn release by human glioma cells.

a, Invasion of sh-c or sh-*TDO* glioma cells into a collagen matrix. **b,** Quantification of the migrated distances of sh-c (open squares) and sh-*TDO* (solid circles) cells into a collagen matrix (n=3, P=0.004, 0.0005 and 0.01 for 24, 48 and 72 h, respectively). **c,** Clonogenic survival of sh-c and sh-*TDO* U87 cells (n=3). **d,** Matrigel boyden chamber assay of normal U87 glioma cells in the absence of Trp, with 70 µM Trp, 30 µM Kyn or 60 mM Kyn (n=3). **e,** Clonogenic survival of LN-18 glioma cells in the absence of Trp, with 70 µM Trp, 30 µM Kyn or 60 µM Kyn (n=3). **f,** Sphere formation of GIC in response to 70 µM Kyn (black bars), controls (white bars) (n=3) **g,** Representative cranial MRIs, H&E and nestin stainings of *CD1 nu/nu* mice implanted with sh-c (upper panel) or sh-*TDO* (lower panel) U87 glioma cells. The images presented are representative of two independent experiments (n=6). **h,** Tumor weight of sh-c (white bars) and sh-*TDO* (black bars) U87 glioma cells injected s.c. in the flank of *CD1 nu/nu* mice, that were treated either with control IgG (IgG) or anti-asialo GM1 antibody (ASIALO) for NK cell depletion (n=8). **i,** Representative sections of the tumors described in **(h)** stained with H&E, (arrows show mitoses, upper panel) and Ki-67 (lower panel).

Figure 4 Kyn activates the AHR. a, Relationship of the 25 genes with the lowest (array) p-values in U87 cells after 8 h of Kyn treatment to the AHR (red: upregulation, green: downregulation). **b,** Translocation of GFP-tagged AHR into the nucleus of mouse hepatoma cells, which do not degrade Trp, after treatment with 50 µM Kyn, 50 µM Trp or 1 nM TCDD, measured after 3 h (neg. control: medium**). c,** Ratios of nuclear to cytoplasmic fluorescent intensity in cells with GFP-tagged AHR after 3 h of indicated treatment (neg. control: medium, pos. control: 1 nM TCDD, 50 µM Kyn). The data distribution is represented by box plots, showing the 25th and 75th percentile together with the median, whiskers represent the

10th and 90th percentile, respectively (*P<0.001, one way ANOVA on ranks, followed by Dunns' method). **d,** AHR Western blots of nuclear and cytoplasmic fractions of control, Kyn-treated and TCDD-treated human LN-229 glioma cells. **e,** Dioxin-responsive element (DRE) chemical activated luciferase gene expression in U87 glioma cells treated with indicated Kyn concentrations. (n=2); TCDD, positive control. **f,** Radioligand binding assay with indicated concentrations of L-3H-Kyn using mouse liver cytosol from *Ahr*-proficient and *Ahr*-deficient mice. Specific binding was calculated by subtracting the radioactivity measured in *Ahr*-deficient cytosol from that of *Ahr*-proficient cytosol. (n=4) **g,** AHR target gene expression in LN-18 glioma cells stimulated with 70 µM Kyn and treated with (black bars) or without (white bars) the AHR antagonist 3,4-dimethoxyflavone (3,4-DMF, 10 µM, n=4). **h,** *CYP1A1* mRNA expression in sh-*AHR* LN-308 glioma cells (black bars) in comparison to controls (sh-c, white bars) treated with 100 µM Kyn, 1 nM TCDD or controls (n=4). **i,** AHR target gene expression in sh-*AHR* LN-308 cells (black bars) in comparison to sh-c cells (white bars, n=4). **j,** mRNA expression of AHR target genes in sh-*TDO* (black bars) U87 glioma cells in comparison to sh-c (white bars, n=4).

Figure 5 The autocrine and paracrine effects of TDO-derived Kyn are mediated via the AHR

a, Migration of sh-c LN-308 glioma cells (white bars) and LN-308 glioma cells with knockdown of the *AHR* by two different shRNAs (sh-*AHR*1, gray bars and sh-*AHR*2 black bars) in the presence or absence of 100 µM Kyn (n=4). **b,** Clonogenic survival of sh-c (white bars) and sh-*AHR* LN-308 glioma cells (black bars) with or without 100 µM Kyn (n=3). **c,** Clonogenic survival of sh-c (white bars) and sh-*AHR* LN-18 cells (black bars, n=3). **d,** Quantification of LCA+ cells stained in human glioma sections with low AHR expression (Histoscore < 150, white bar, n=10) and in human glioma sections with high AHR expression (Histoscore ≥ 150, black bar, n=12). **e,** Quantification of CD8+ cells stained in human glioma

sections with low AHR expression (Histoscore < 150, white bar, n=8) and in human glioma sections with high AHR expression (Histoscore ≥ 150, black bar, n=12). **f,** Immunofluorescence stainings of LCA and TIPARP in human glioma sections with low or high TDO expression. **g,** Tumor weight measured 15 days after s.c. injection of murine GL261 glioma cells with and without *Tdo* expression in the flanks of *Ahr*-proficient (white bars) or *Ahr*-deficient mice (black bars, n=6). **h,** Representative **s**tainings of LCA+ immune cells in the subcutaneous GL261 tumors described above. **i,** Quantification of LCA+ immune cells stained in the subcutaneous *Tdo*-proficient and *Tdo*-deficient GL261 tumors in *Ahr*-proficient and *Ahr*-deficient mice presented using box plots, showing the 25th and 75th percentile and the median, whiskers represent the 10th and 90th percentile, respectively (n=4). **j,** Growth of *AHR*-proficient (solid circles) and *AHR*-deficient (open circles) human LN-308 glioma cells injected s.c. into the flank of *CD1nu/nu* mice was monitored using metric callipers (n=7). Tumor weight was calculated using the equation: tumor weight (g) = (length (cm) × width $(cm)^2$) × 0.5. For statistical analysis see Supplementary note 18. **k,** Representative stainings of the subcutaneous *AHR*-proficient (sh-c) and *AHR*-deficient (sh-*AHR*) LN-308 tumors with H&E (arrows indicate mitoses), and for AHR expression as well as Ki-67 expression.

Figure 6 TDO-derived Kyn activates the AHR in diverse human cancers and AHR activation predicts survival in glioma patients

a, Correlation of TDO expression (red) and AHR expression (brown) in consecutive sections of human glioblastoma tissue. Arrows indicate vessels for orientation. Magnification 40x, insets 200x. **b,** Correlation of TDO expression and AHR target gene (CYP1A1) expression in diffuse astrocytoma (left) and glioblastoma (right). Magnification 40x, insets 200x. **c,** Correlation between TDO and AHR expression in human glioma tissue based on H-scores of TDO and AHR, calculated using Spearman rank correlation (n=26). **d,** Correlation between

TDO and *CYP1B1* expression in microarray data of human glioblastoma (n=396) analysed by Spearman rank correlation. **e,** Correlation between *TDO* and *CYP1B1* expression in microarray data of human bladder cancer (left, n=58), human lung cancer (middle, n=122) and human ovarian carcinoma (right, n=91) analysed by Spearman rank correlation. **f,** Survival probabilities of glioma patients (WHO grade II-IV) with an upregulated expression (red) of *TDO* or the *AHR* compared to patients with intermediate (blue) or downregulated (green) expression of these genes derived from Rembrandt. For statistical analysis see Supplementary note 13. **g,** Survival probabilities of glioblastoma patients with an upregulated expression (red) of the AHR target gene *CYP1B1* compared to patients with downregulated (green) expression of *CYP1B1* derived from the glioblastoma data set of The Cancer Genome Atlas (TCGA) network (n=362). **h,** Synoptical figure highlighting the autocrine and paracrine effects of TDO-derived Kyn on cancer cells and immune cells via the AHR.

Figure 1

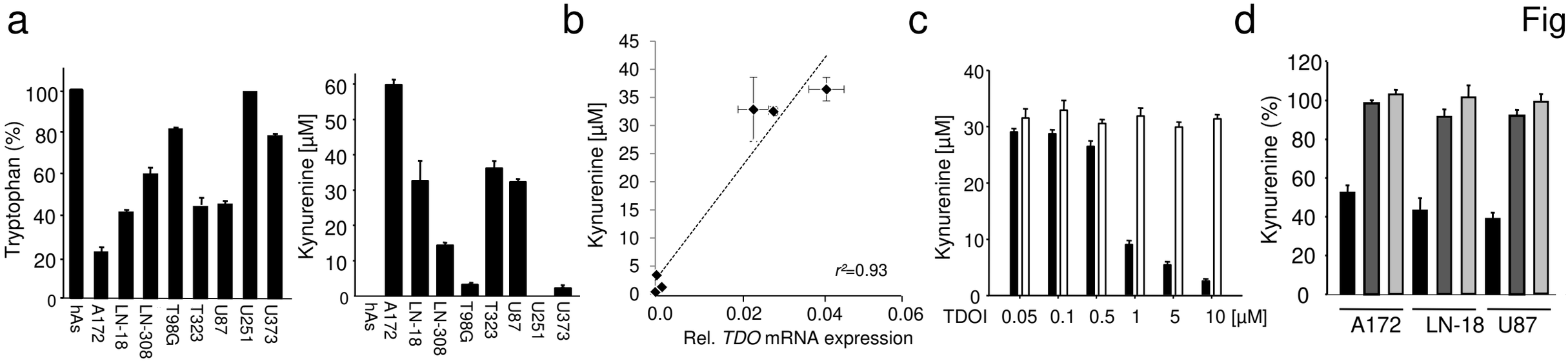
a
Tryptophan (%)
hAs
A172
LN-18
LN-308
T98G
T323
U87
U251
U373
Kynurenine [µM]
b
Kynurenine [µM]
r^2=0.93
Rel. *TDO* mRNA expression
c
Kynurenine [µM]
TDOI 0.05 0.1 0.5 1 5 10 [µM]
d
Kynurenine (%)
A172 LN-18 U87

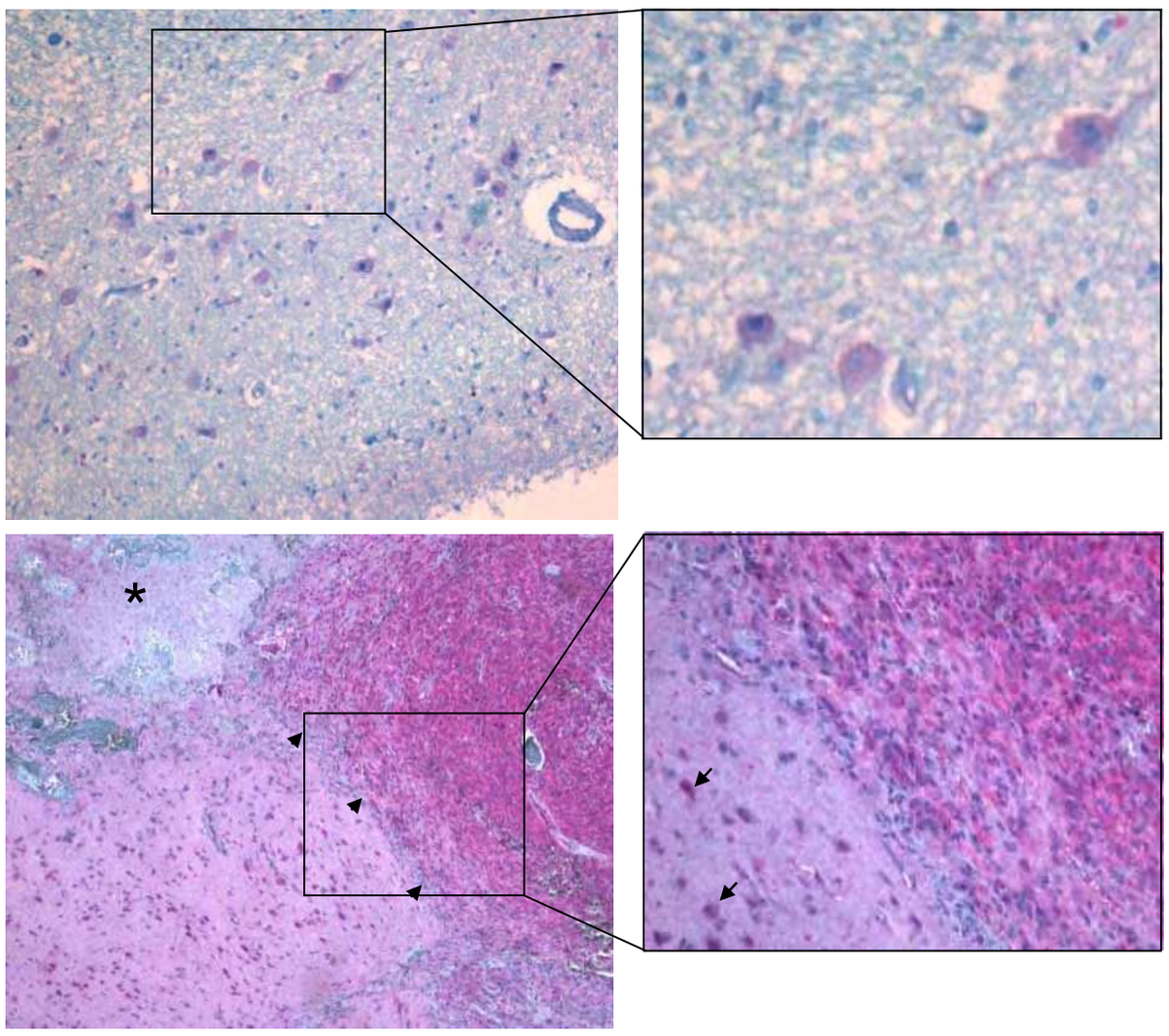
e
*

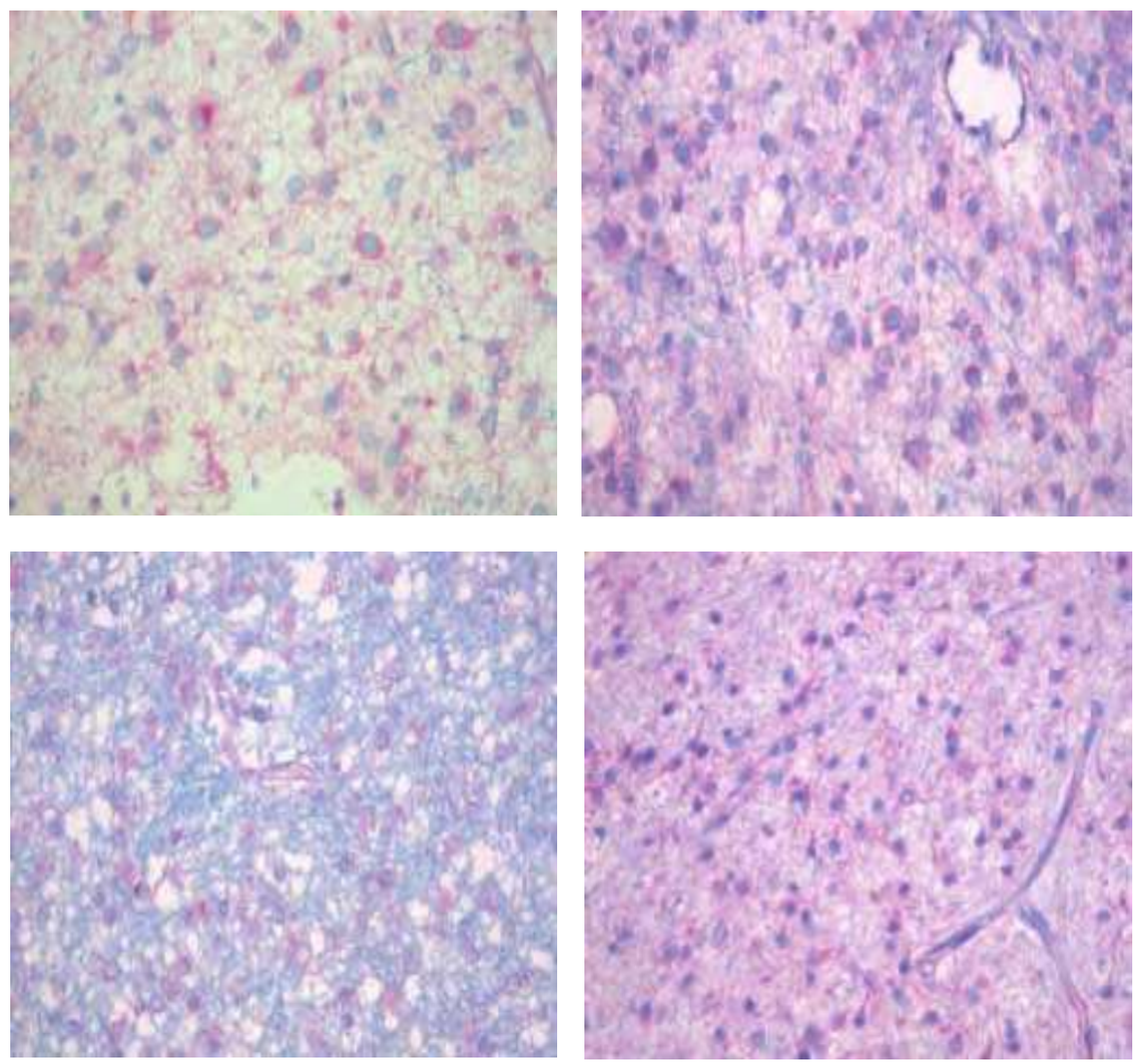
f

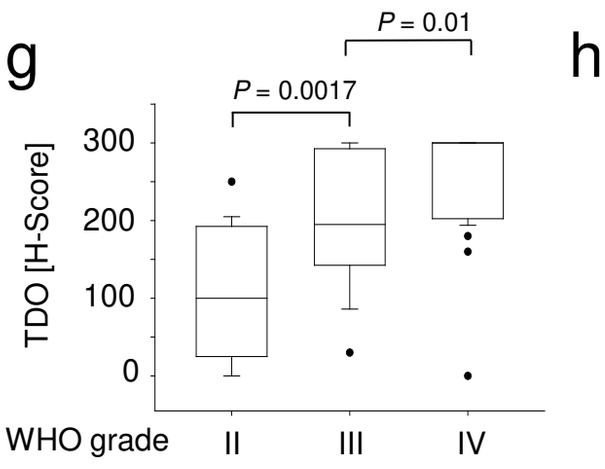
g
P = 0.01
P = 0.0017
TDO [H-Score]
WHO grade II III IV

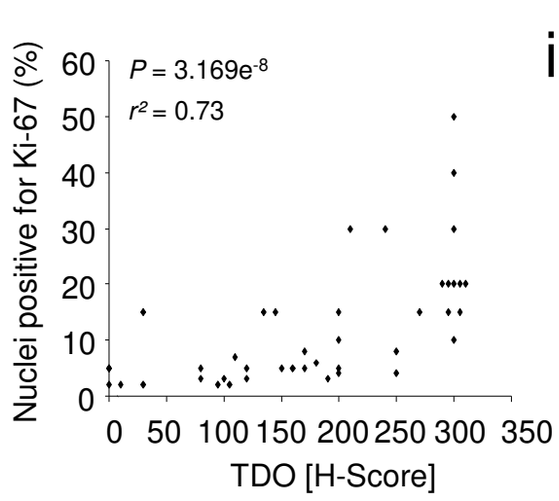
h
P = 3.169e-8
r² = 0.73
Nuclei positive for Ki-67 (%)
TDO [H-Score]

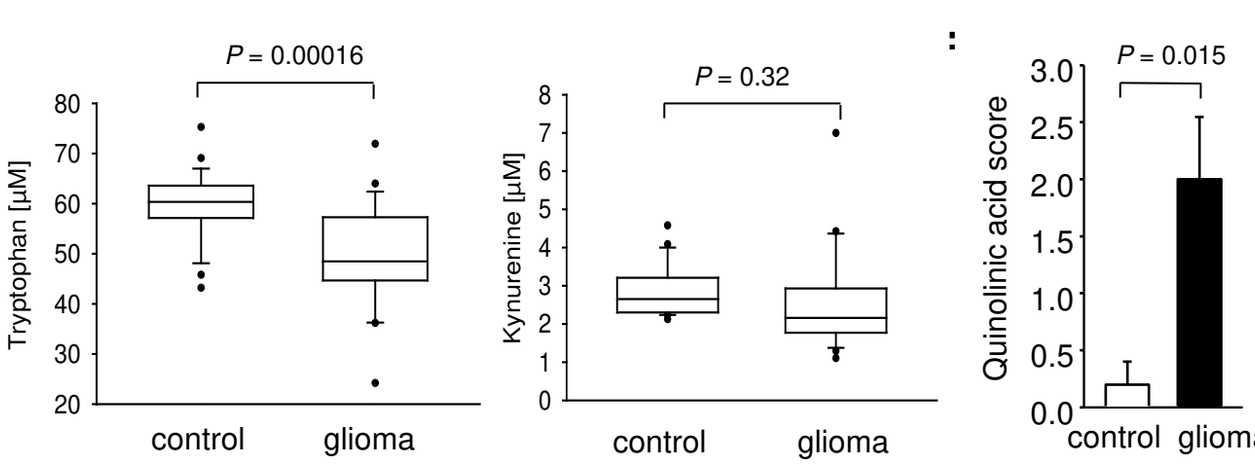
i
P = 0.00016
Tryptophan [µM]
control glioma
P = 0.32
Kynurenine [µM]
control glioma
P = 0.015
Quinolinic acid score
control glioma

Figure 2

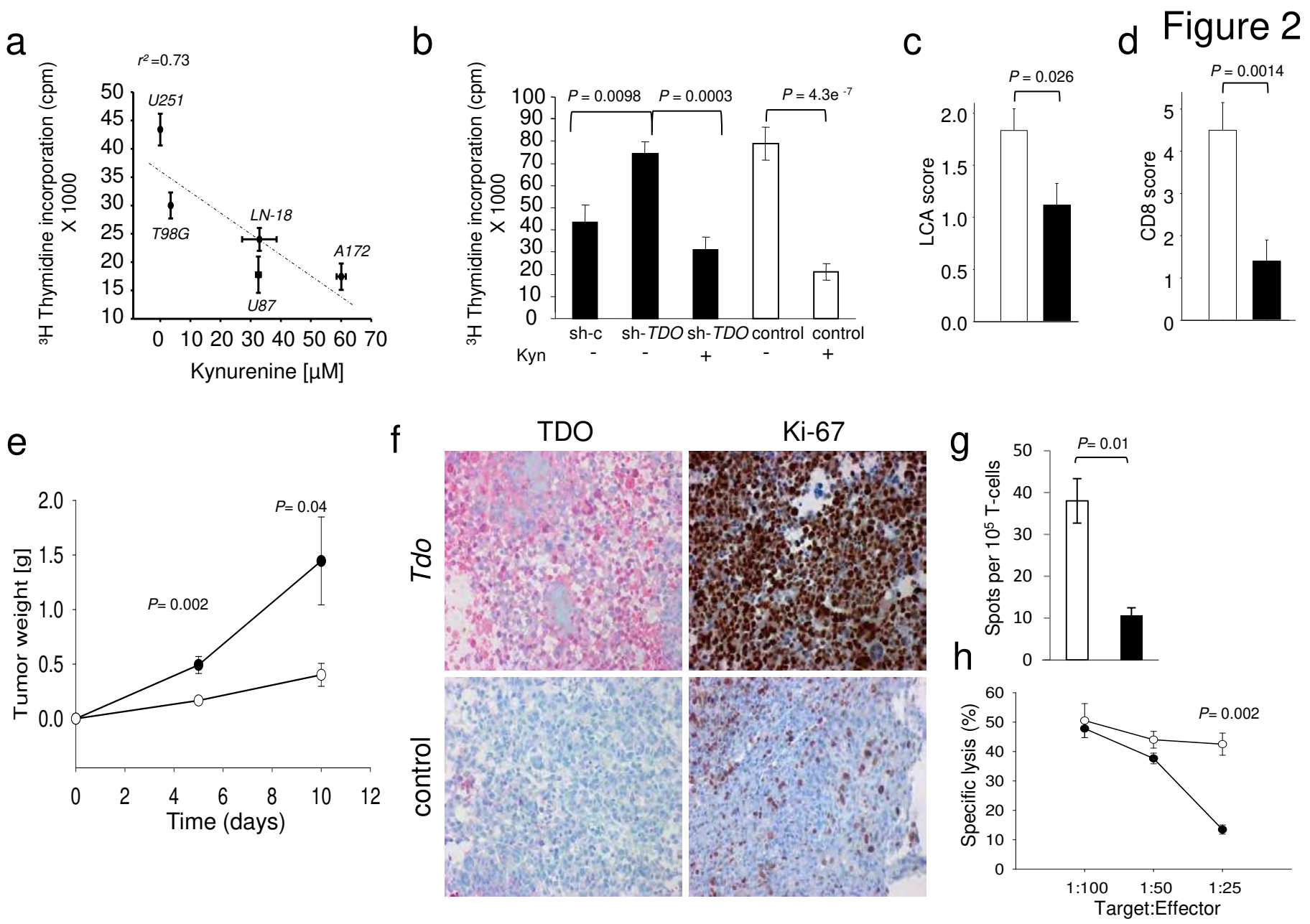
a
r² =0.73
U251
T98G
LN-18
U87
A172
³H Thymidine incorporation (cpm) X 1000
Kynurenine [μM]
b
P = 0.0098
P = 0.0003
P = 4.3e -7
³H Thymidine incorporation (cpm) X 1000
sh-c
sh-TDO
sh-TDO
control
control
Kyn
c
P = 0.026
LCA score
d
P = 0.0014
CD8 score
e
P= 0.04
P= 0.002
Tumor weight [g]
Time (days)
f
TDO
Ki-67
Tdo
control
g
P= 0.01
Spots per 10⁵ T-cells
h
P= 0.002
Specific lysis (%)
1:100
1:50
1:25
Target:Effector

Figure3

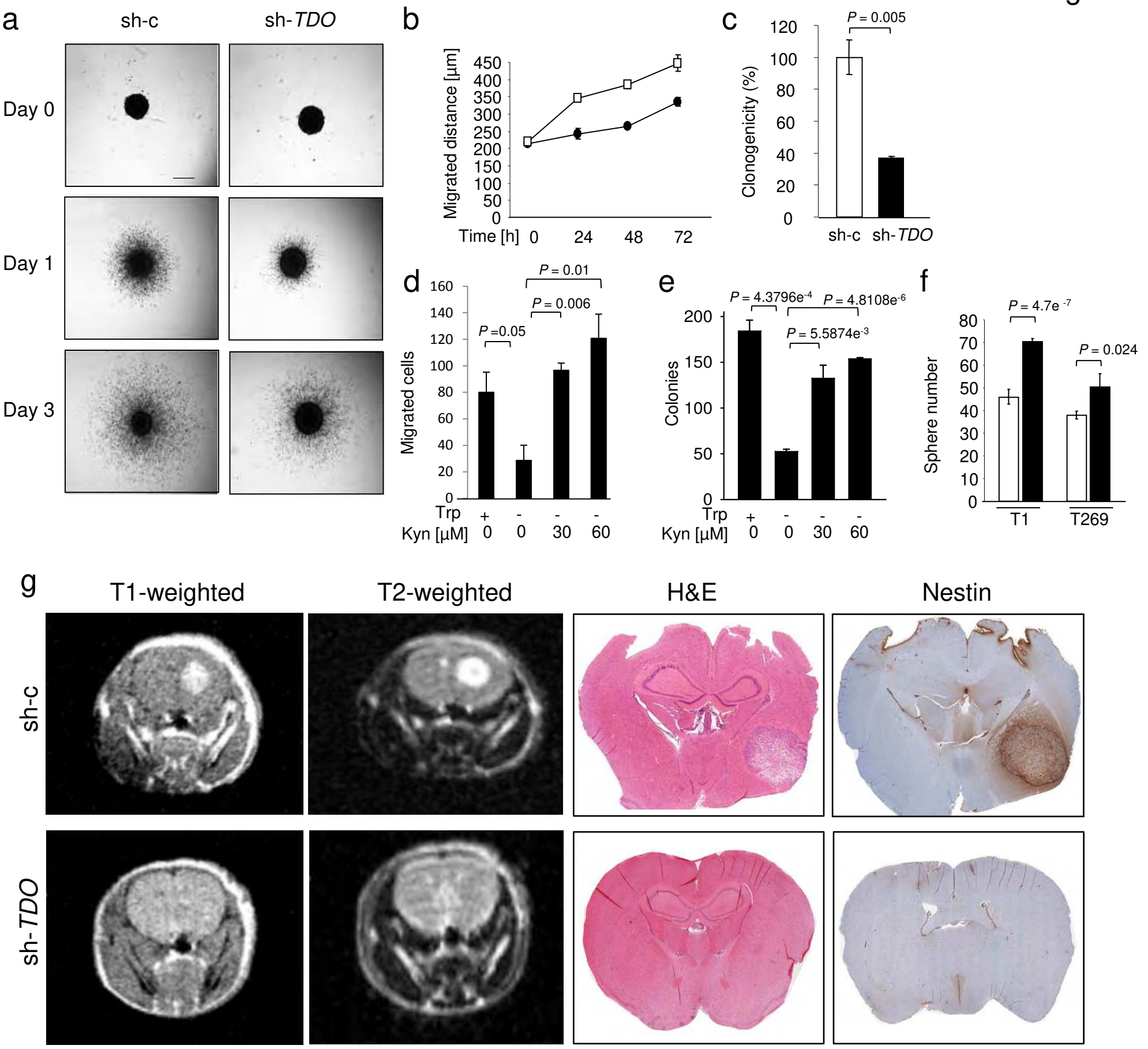
a
sh-c
sh-TDO
Day 0
Day 1
Day 3
b
Migrated distance [μm]
Time [h] 0 24 48 72
c
P = 0.005
Clonogenicity (%)
sh-c sh-TDO
d
P = 0.01
P = 0.006
P =0.05
Migrated cells
Trp + - - -
Kyn [μM] 0 0 30 60
e
P = 4.3796e-4
P = 4.8108e-6
P = 5.5874e-3
Colonies
Trp + - - -
Kyn [μM] 0 0 30 60
f
P = 4.7e -7
P = 0.024
Sphere number
T1
T269
g
T1-weighted
T2-weighted
H&E
Nestin
sh-c
sh-TDO
h
P= 0.0002
P= 0.001
P= 0.03
Tumor weight [mg]
IgG ASIALO IgG ASIALO
sh-c
sh-TDO
i
sh-c ASIALO
sh-c control
sh-TDO ASIALO
sh-TDO control
H&E
Ki-67

Figure4

a

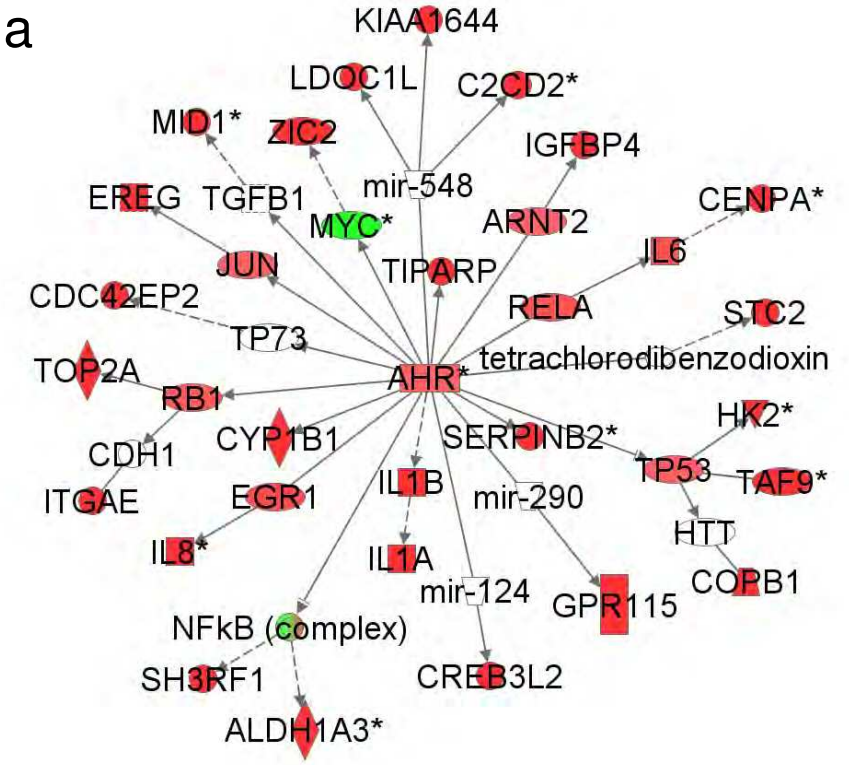

b

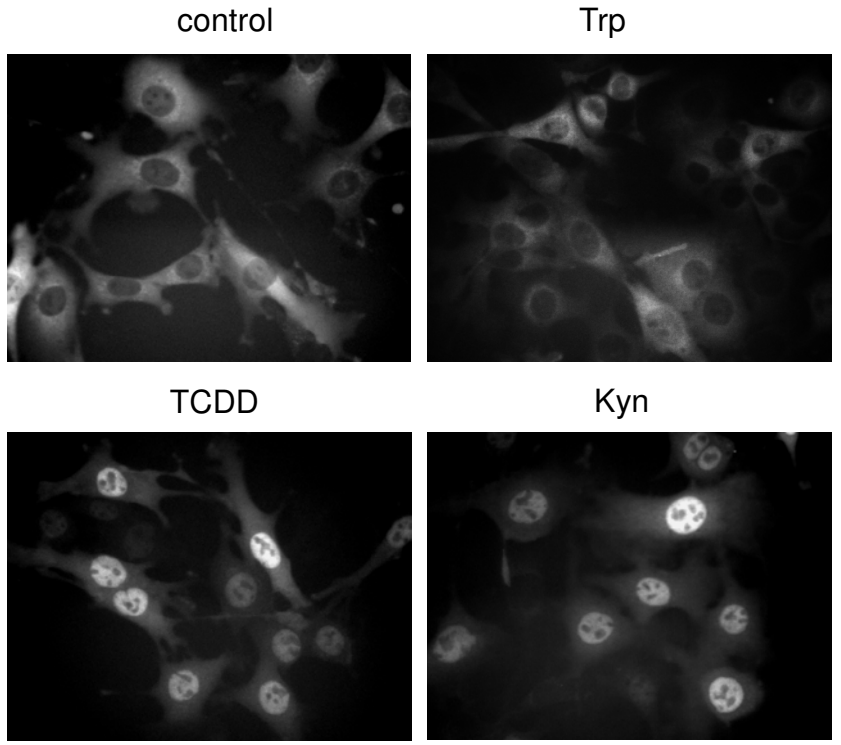

c

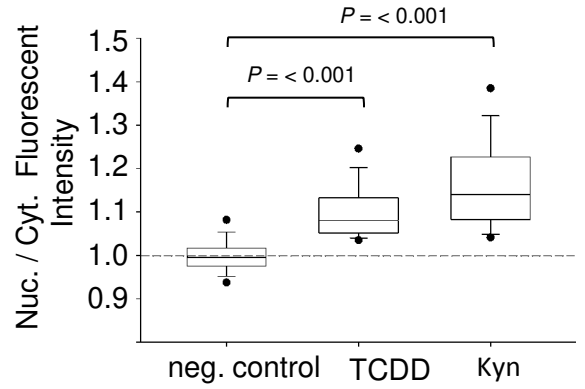

d

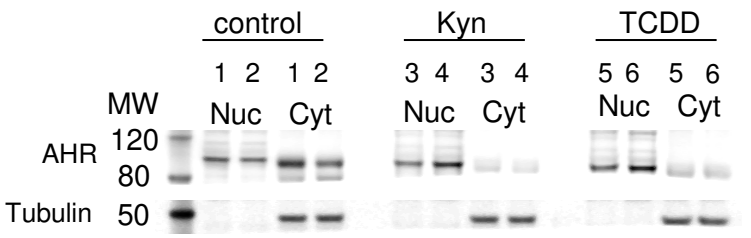

e

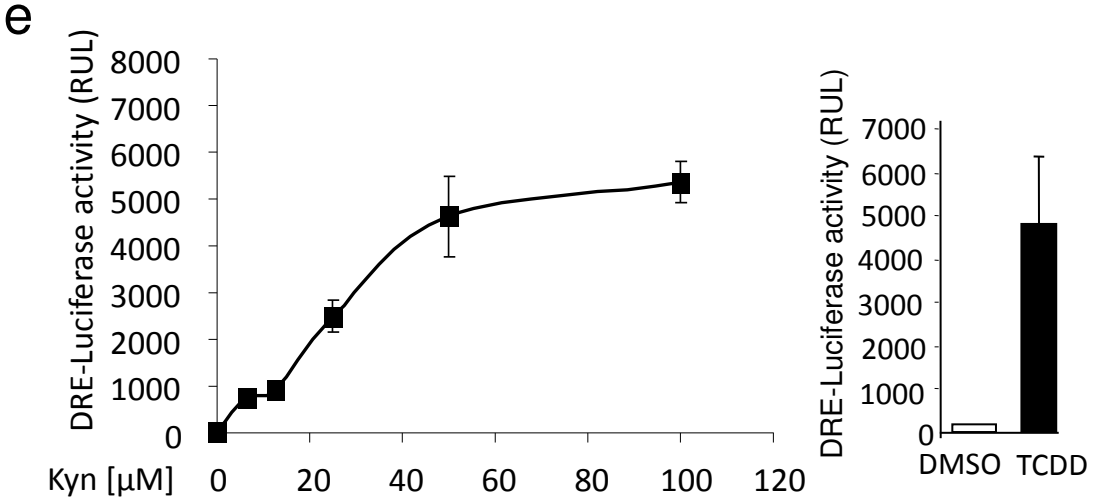

f

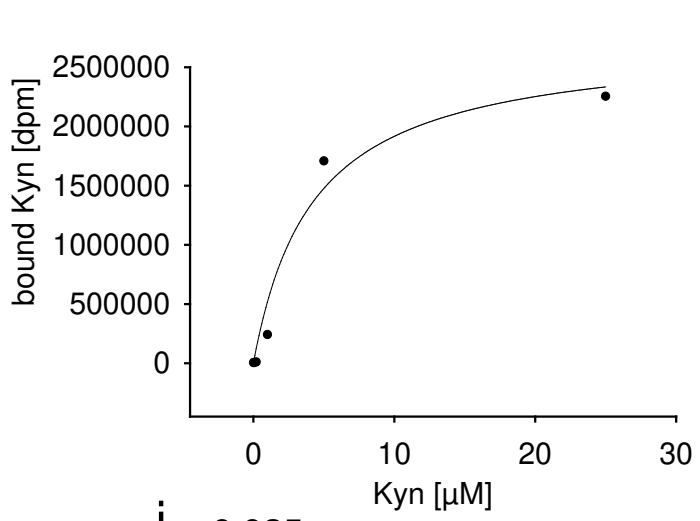

g

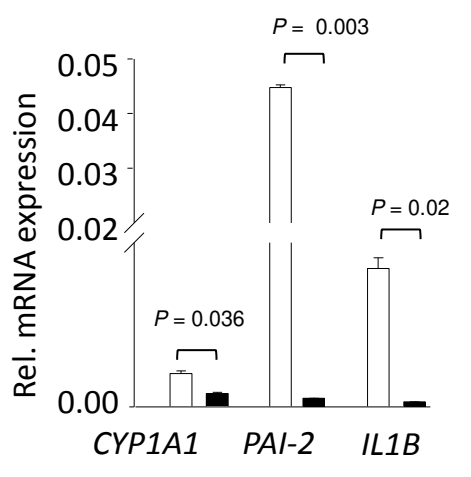

h

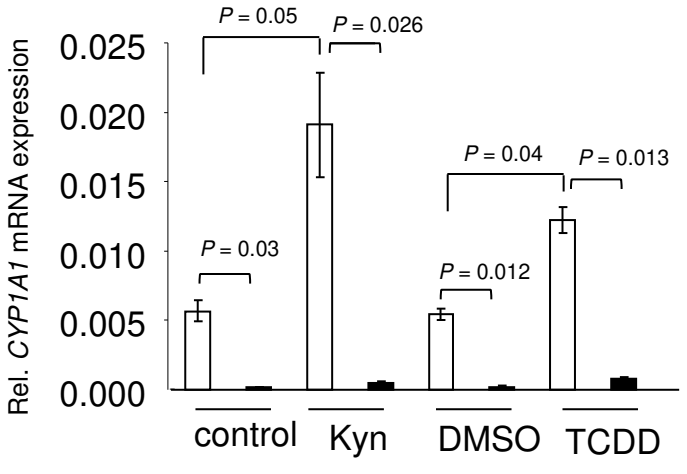

i

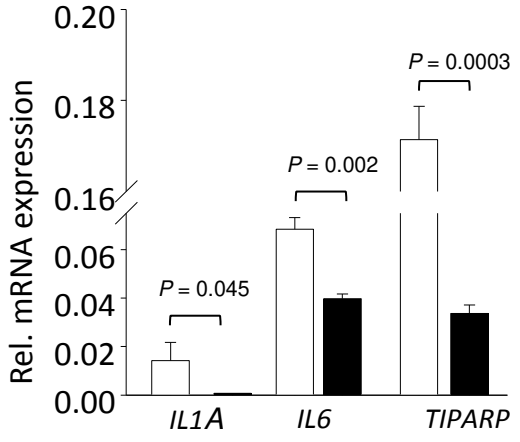

j

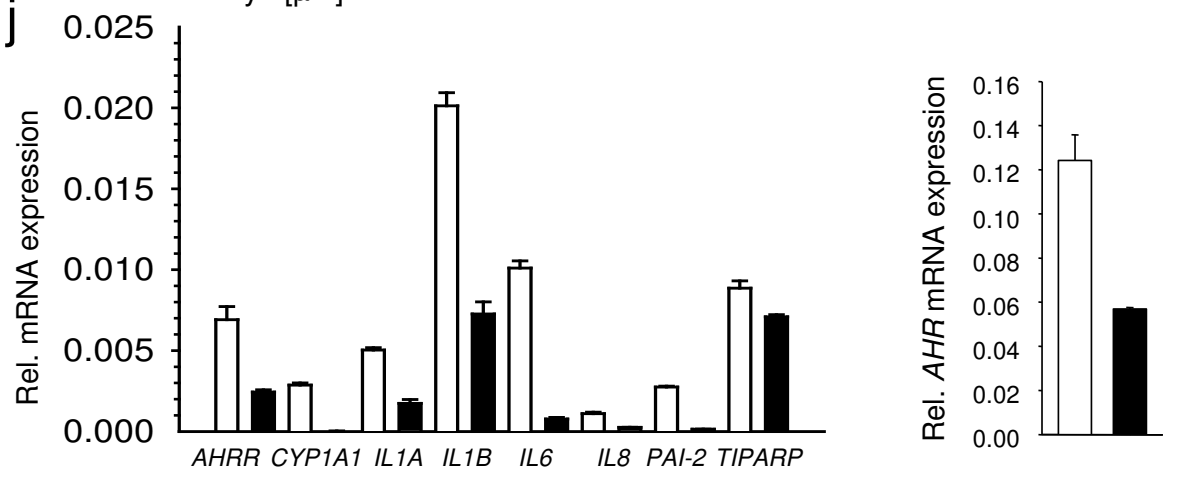

Figure 5

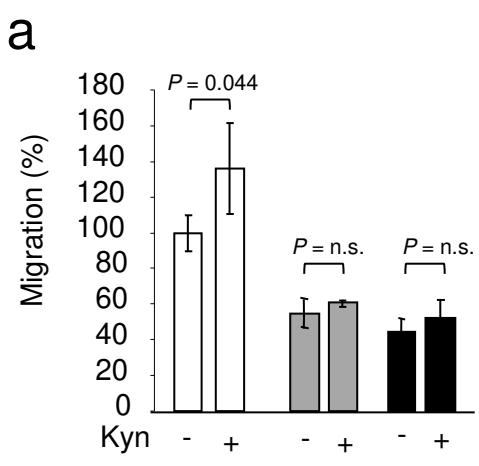
a
Migration (%)
P = 0.044
P = n.s.
P = n.s.
Kyn - + - + - +

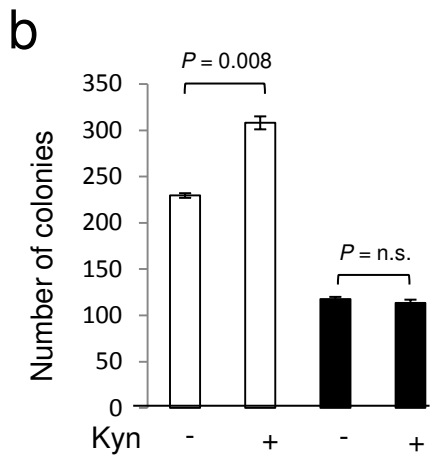
b
Number of colonies
P = 0.008
P = n.s.
Kyn - + - +

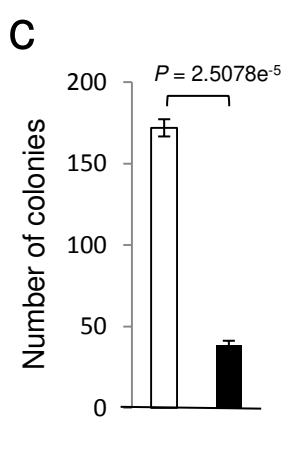
c
Number of colonies
P = 2.5078e-5

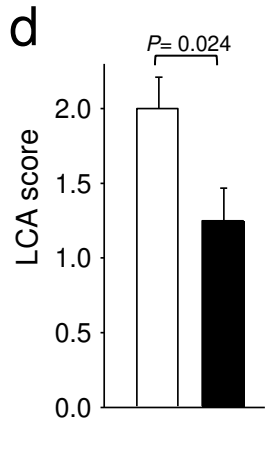
d
LCA score
P= 0.024

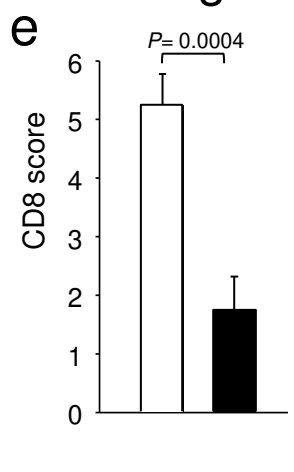
e
CD8 score
P= 0.0004

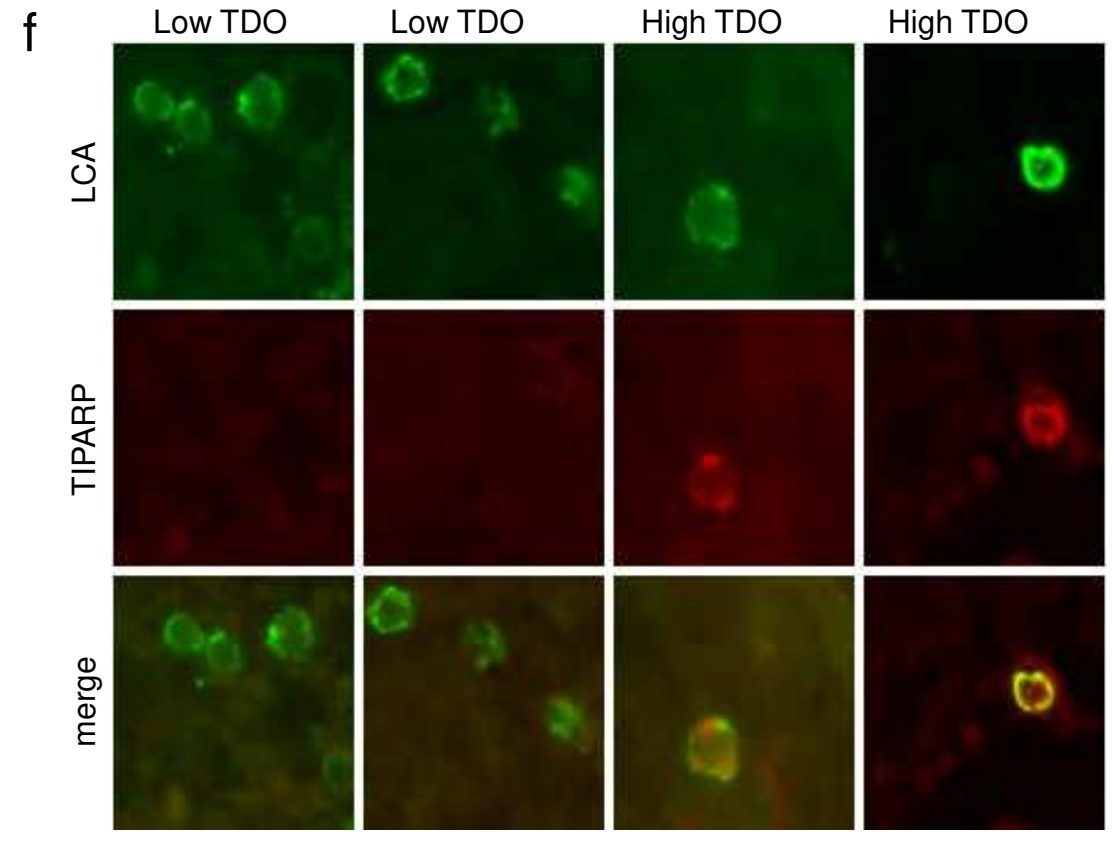
f
Low TDO
Low TDO
High TDO
High TDO
LCA
TIPARP
merge

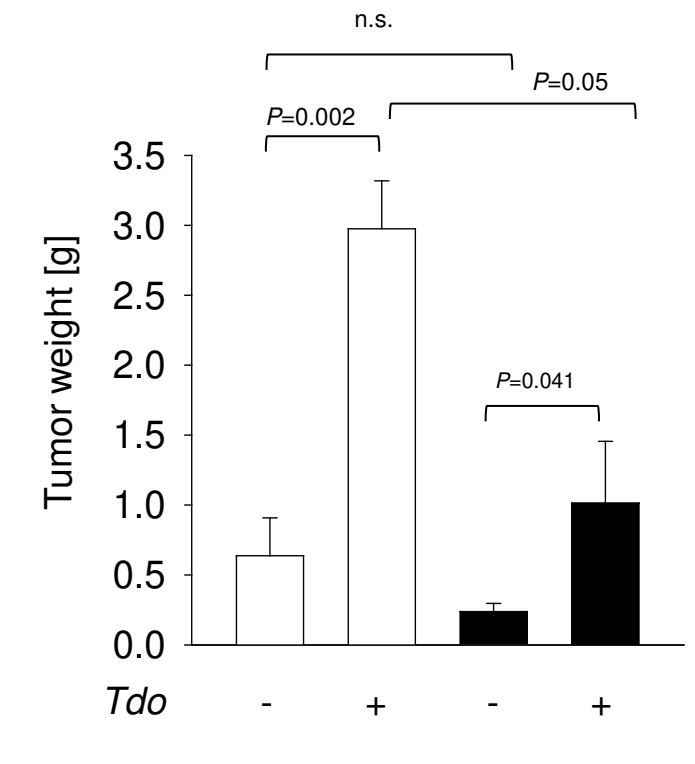
g
n.s.
P=0.05
P=0.002
P=0.041
Tumor weight [g]
Tdo - + - +

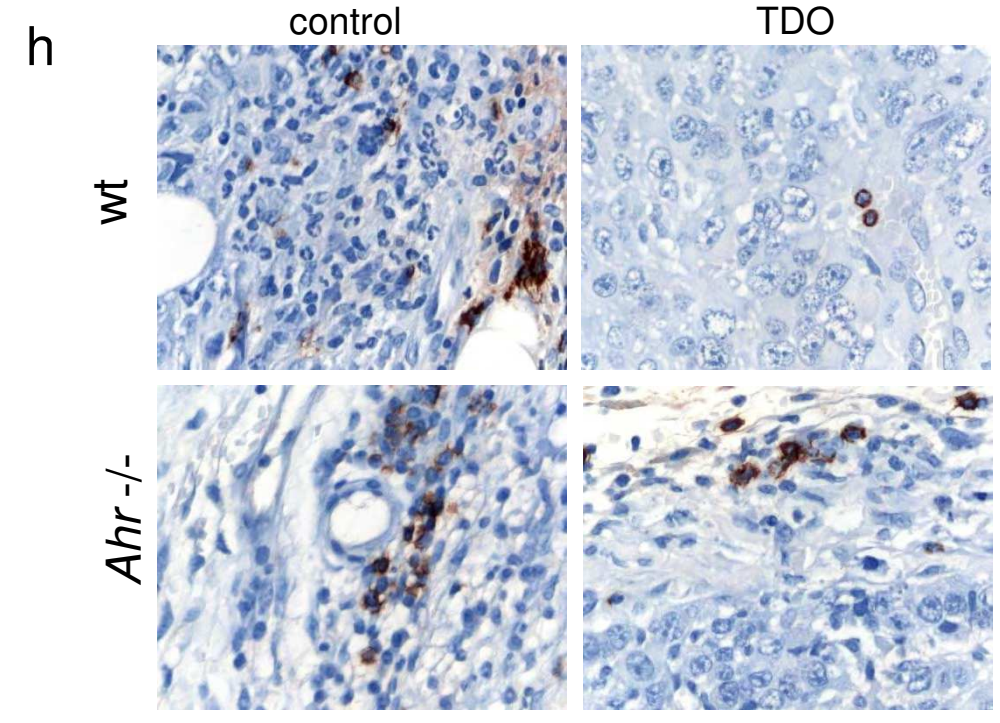
h
control
TDO
wt
Ahr -/-

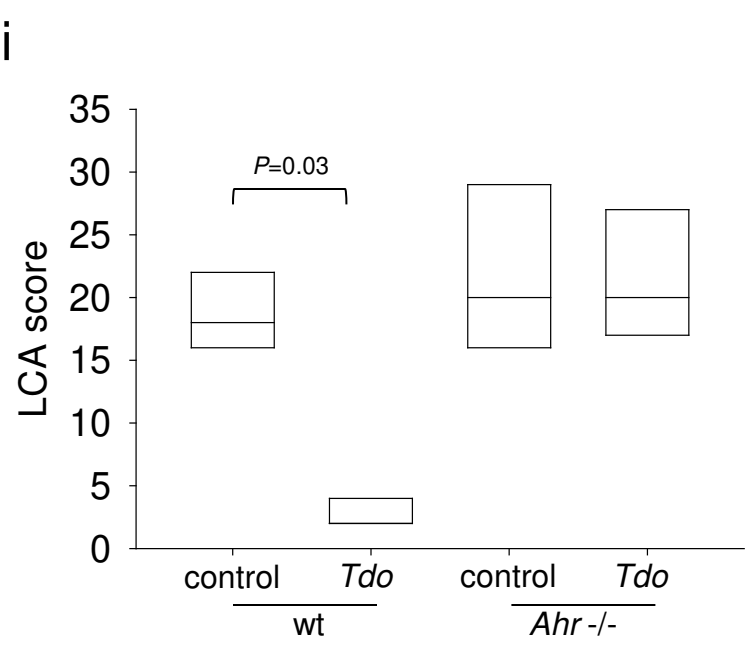
i
LCA score
P=0.03
control
Tdo
control
Tdo
wt
Ahr -/-

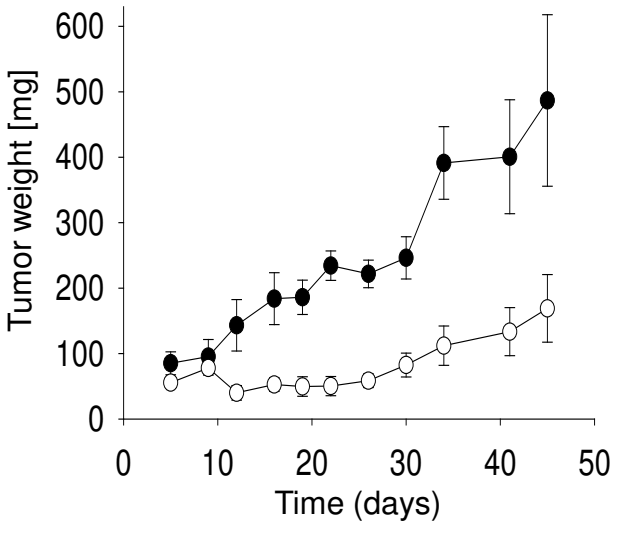
j
Tumor weight [mg]
Time (days)

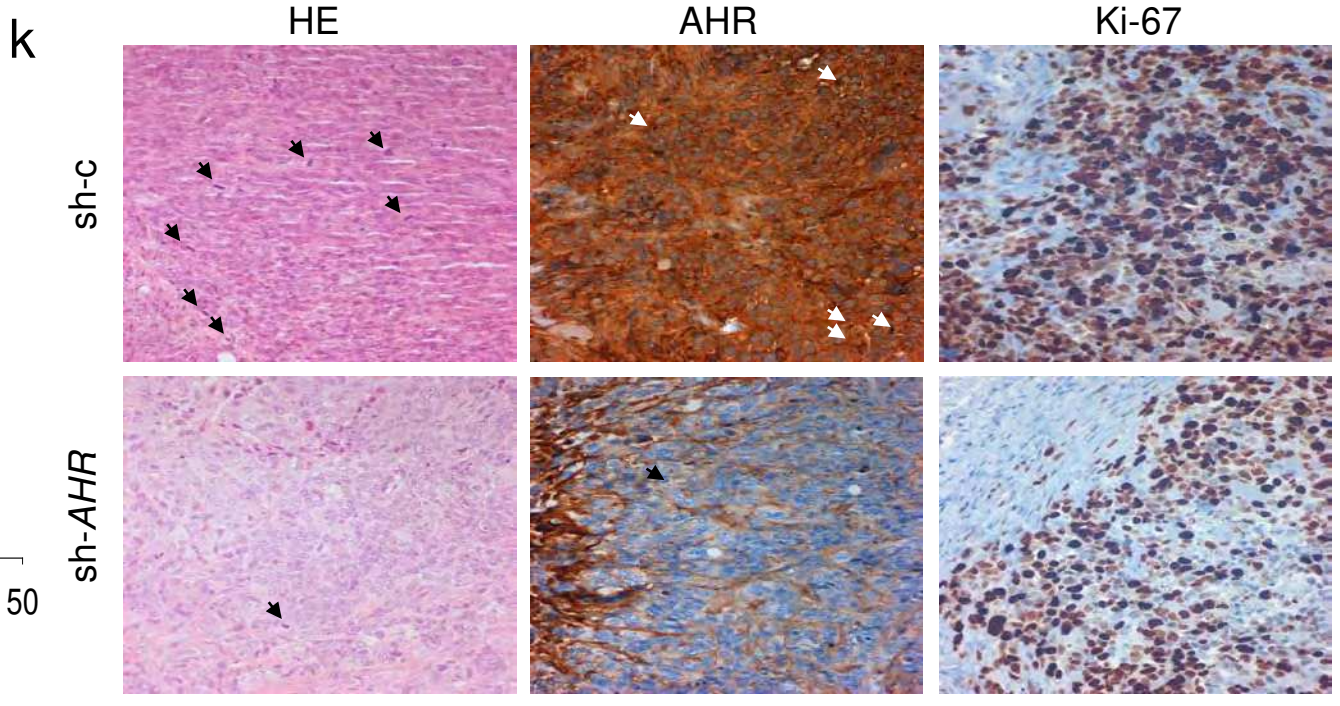
k
HE
AHR
Ki-67
sh-c
sh-AHR

Figure6

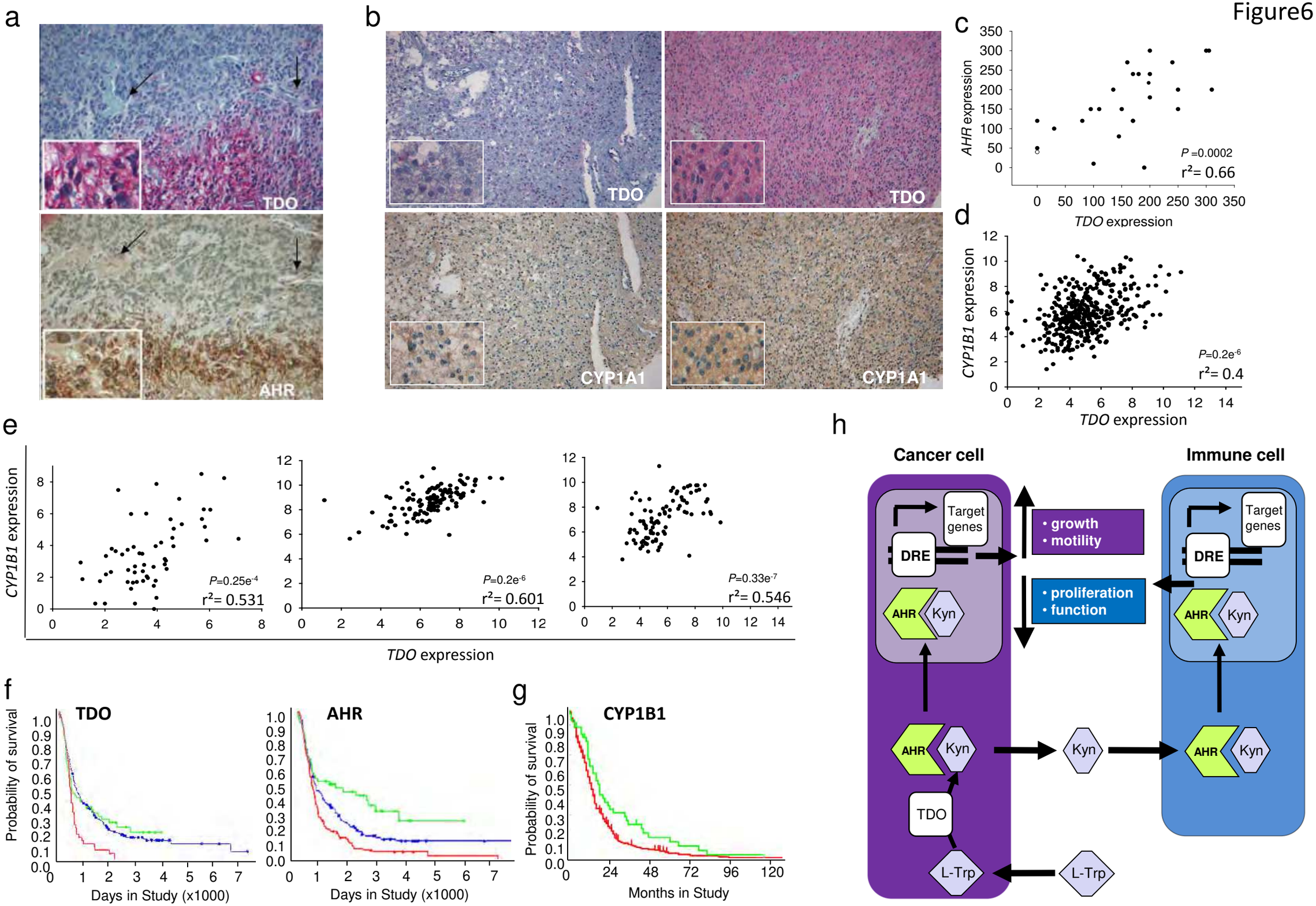
a
TDO
AHR
b
TDO
TDO
CYP1A1
CYP1A1
c
AHR expression
TDO expression
P =0.0002
r²= 0.66
d
CYP1B1 expression
TDO expression
P=0.2e-6
r²= 0.4
e
CYP1B1 expression
P=0.25e-4
r²= 0.531
P=0.2e-6
r²= 0.601
P=0.33e-7
r²= 0.546
TDO expression
f
TDO
AHR
Probability of survival
Days in Study (x1000)
Days in Study (x1000)
g
CYP1B1
Probability of survival
Months in Study
h
Cancer cell
Immune cell
Target genes
DRE
AHR
Kyn
• growth
• motility
• proliferation
• function
TDO
L-Trp
L-Trp